



OPEN ACCESS

EDITED BY

Wei Xu,
Fudan University, China

REVIEWED BY

Michele Kay Anderson,
University of Toronto, Canada
Jaydeep Bhat,
Ruhr University Bochum, Germany

*CORRESPONDENCE

Cristina Hernández-Munain
chmunain@ipb.csic.es

[†]These authors share first authorship

SPECIALTY SECTION

This article was submitted to
T Cell Biology,
a section of the journal
Frontiers in Immunology

RECEIVED 13 May 2022

ACCEPTED 03 August 2022

PUBLISHED 19 August 2022

CITATION

Rodríguez-Caparrós A, Tani-ichi S,
Casal Á, López-Ros J, Suñé C, Ikuta K
and Hernández-Munain C (2022)
Interleukin-7 receptor signaling is
crucial for enhancer-dependent TCR δ
germline transcription mediated
through STAT5 recruitment.
Front. Immunol. 13:943510.
doi: 10.3389/fimmu.2022.943510

COPYRIGHT

© 2022 Rodríguez-Caparrós, Tani-ichi,
Casal, López-Ros, Suñé, Ikuta and
Hernández-Munain. This is an open-
access article distributed under the
terms of the [Creative Commons
Attribution License \(CC BY\)](https://creativecommons.org/licenses/by/4.0/). The use,
distribution or reproduction in other
forums is permitted, provided the
original author(s) and the copyright
owner(s) are credited and that the
original publication in this journal is
cited, in accordance with accepted
academic practice. No use,
distribution or reproduction is
permitted which does not comply with
these terms.

Interleukin-7 receptor signaling is crucial for enhancer-dependent TCR δ germline transcription mediated through STAT5 recruitment

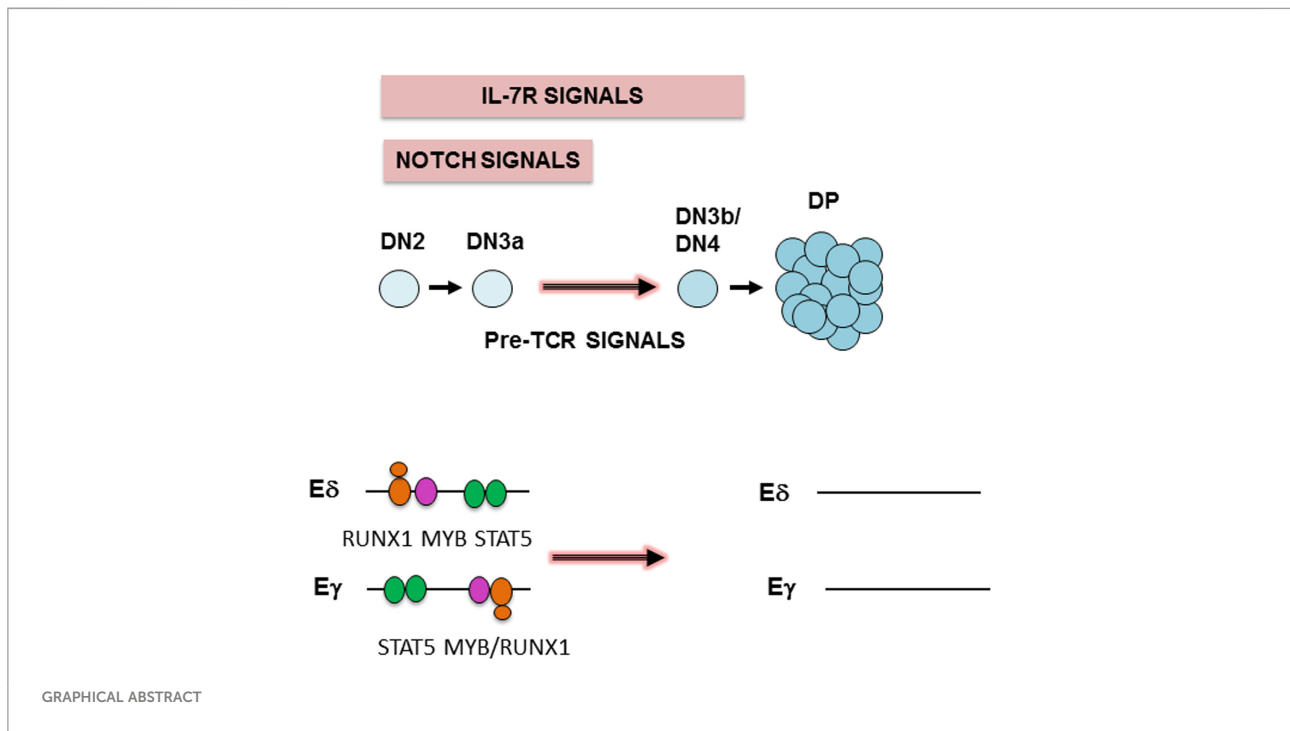
Alonso Rodríguez-Caparrós^{1†}, Shizue Tani-ichi^{2†}, Áurea Casal¹, Jennifer López-Ros¹, Carlos Suñé¹, Koichi Ikuta² and Cristina Hernández-Munain^{1*}

¹Institute of Parasitology and Biomedicine "López-Neyra"- Spanish Scientific Research Council (IPBLN-CSIC), Technological Park of Health Sciences (PTS), Granada, Spain, ²Laboratory of Immune Regulation, Department of Virus Research, Institute for Life and Medical Sciences, Kyoto University, Kyoto, Japan

$\gamma\delta$ T cells play important roles in immune responses by rapidly producing large quantities of cytokines. Recently, $\gamma\delta$ T cells have been found to be involved in tissue homeostatic regulation, playing roles in thermogenesis, bone regeneration and synaptic plasticity. Nonetheless, the mechanisms involved in $\gamma\delta$ T-cell development, especially the regulation of TCR δ gene transcription, have not yet been clarified. Previous studies have established that NOTCH1 signaling plays an important role in the *Tcrq* and *Tcrd* germline transcriptional regulation induced by enhancer activation, which is mediated through the recruitment of RUNX1 and MYB. In addition, interleukin-7 signaling has been shown to be required for *Tcrq* germline transcription, V γ J γ rearrangement and $\gamma\delta$ T-lymphocyte generation as well as for promoting T-cell survival. In this study, we discovered that interleukin-7 is required for the activation of enhancer-dependent *Tcrd* germline transcription during thymocyte development. These results indicate that the activation of both *Tcrq* and *Tcrd* enhancers during $\gamma\delta$ T-cell development in the thymus depends on the same NOTCH1- and interleukin-7-mediated signaling pathways. Understanding the regulation of the *Tcrd* enhancer during thymocyte development might lead to a better understanding of the enhancer-dependent mechanisms involved in the genomic instability and chromosomal translocations that cause leukemia.

KEYWORDS

enhancer, transcription, T-cell receptor, T-cell development, V(D)J recombination, IL-7, STAT5, $\gamma\delta$ T cells



Introduction

$\gamma\delta$ T cells constitute a minor T-cell population (1-10% of all T lymphocytes) compared with canonical $\alpha\beta$ T cells (1). In addition to blood and secondary immune organs, where $\alpha\beta$ T cells reside, $\gamma\delta$ T cells accumulate in the gut mucosa, lung, skin, uterus, adipose tissue, meninges, liver and peritoneal cavity, playing important roles in the initiation and propagation of immune responses. During antigen recognition, $\gamma\delta$ T cells express a T-cell receptor (TCR), TCR $\gamma\delta$, which can specifically respond to a variety of ligands, including nonpeptidic antigens, such as phosphoantigens and lipids that are not presented by major histocompatibility complex molecules, and peptides presented by the major histocompatibility complex (2, 3). In addition, $\gamma\delta$ T-cell immune functions include (i) rapid production of large quantities of cytokines, (ii) killing of infected and tumor cells in a manner similar to natural killer cells, (iii) elimination of bacteria and other particles, and (iv) antigen presentation (1). Due to their innate and adaptive properties that enable them to robustly kill a wide range of tumor or infected cells, ability to present peptide antigens to $\alpha\beta$ T cells, and major histocompatibility complex-independent antigen recognition, increased interest has recently been directed to their potential use in novel immunotherapies (2). In addition, important roles played by $\gamma\delta$ T cells, including their functions in thermogenesis, bone regeneration, and synaptic plasticity, have been identified in tissue homeostasis (4–8). Despite the growing interest in these cells, the mechanism by

which TCR δ gene transcription is regulated during $\gamma\delta$ T-cell generation has not yet been clarified.

During development in the thymus, T-cell precursors transition through a series of stages in which CD4 and CD8 are differentially expressed; these intermediates include CD4⁻CD8⁻ double-negative (DN), CD4⁺CD8⁺ double-positive (DP), and CD4⁺ or CD8⁺ single-positive (SP) thymocytes (9). Four DN populations, DN1 to DN4, are distinguished by the expression of CD25 and CD44; DN2 and DN3 thymocytes can be further classified into DN2a and DN2b and DN3a and DN3b, based on the expression of CD117 and CD27, respectively (9, 10).

Ordered expression of TCR $\gamma\delta$ and TCR $\alpha\beta$ during thymocyte development is highly controlled to ensure the correct development of $\gamma\delta$ and $\alpha\beta$ T cells. TCR γ and TCR δ chains are simultaneously expressed in DN2b and DN3a thymocytes to generate TCR $\gamma\delta$. The TCR β chain is expressed in DN3a thymocytes with an invariable pre-T α chain, resulting in a TCR precursor known as pre-TCR, which induces cell proliferation, CD4 and CD8 expression leading to DP thymocyte generation, and TCR α chain expression. TCR α and TCR β chains are then simultaneously expressed in DP and SP thymocytes to form TCR $\alpha\beta$. Therefore, $\gamma\delta$ T cells arise from DN2b and DN3a thymocytes as a result of TCR $\gamma\delta$ expression, whereas $\alpha\beta$ T cells are derived from DP thymocytes as a result of TCR $\alpha\beta$ expression. Because TCR γ , TCR δ and TCR β rearrangements occur in bipotent $\alpha\beta/\gamma\delta$ T-cell precursors, the final outcomes derived from these events have an

unquestionable impact on the ultimate T-cell fate ($\alpha\beta$ vs. $\gamma\delta$ T-cell), which is regulated by an instructive mechanism based on the stronger signaling of TCR $\gamma\delta$ than that mediated by the pre-TCR (11–13). Interestingly, pre-TCR signaling not only induces the expression of the TCR α chain but also induces the termination of TCR γ and TCR δ chain expression (14–16). Therefore, the exact control of the expression of these chains is crucial for the normal assembly of functional TCRs in thymocytes and the generation of $\gamma\delta$ and $\alpha\beta$ T cells (9, 17).

The ordered expression of the different TCR chains during thymocyte development depends on the specific regulation of enhancer-dependent germline transcription and V(D)J recombination at each individual TCR gene (9). These genes exist in two different conformations, unrearranged and rearranged, with a correctly rearranged configuration required for the expression of a functional chain (9). To pass from an unrearranged to a rearranged configuration, the enhancers present within the TCR genes play a critical role by triggering noncoding germline transcription initiated at the D and J gene segment promoters to promote accessibility of RAG proteins to the D-J region (18–20). V(D)J recombination-deficient mice, such as RAG-deficient mice, have a total block at the DN3a stage due to their inability to rearrange and express any of their TCR chains, as CD27 expression is dependent on intracellular TCR β expression (10, 21). After rearrangement, transcription at the rearranged TCR genes depends on enhancer-dependent activation of the recombined V gene segment.

Expression of the TCR γ and TCR δ chains depends on the activity of their respective transcriptional enhancers, E γ and E δ , which activate germline transcription of their unrearranged respective gene and subsequent recombination in DN2b to DN3a thymocytes (22, 23). Successful V γ J γ and V δ D δ J δ rearrangements (Figure S1) permit the expression of TCR $\gamma\delta$ in these cells, which drives thymocyte differentiation into $\gamma\delta$ T lymphocytes (10). Because *Tcrg*, *Tcrd*, and *Tcrb* germline transcription and recombination occur before TCR $\gamma\delta$ or pre-TCR expression in bipotent $\alpha\beta/\gamma\delta$ T-cell precursors, these events are not directly involved in $\alpha\beta$ vs. $\gamma\delta$ T-lineage determination, which depends on the expression of TCR $\gamma\delta$ and pre-TCR (11–13). In DP thymocytes, *Tcrg* and *Tcrd* transcription is inactivated by pre-TCR signaling (14–16, 23).

Signaling mediated through NOTCH1 and interleukin-7 (IL-7) receptor (IL-7R) is essential for the generation of T cells (24). NOTCH1 signaling is indispensable for T-cell commitment at the DN2a thymocyte stage, and IL-7R signaling is required for thymocyte survival, proliferation and maturation and ultimately the generation of $\gamma\delta$ T cells (25–28). Interestingly, the NOTCH1 and IL-7R signaling pathways constitute part of a transcriptional regulatory axis, in which IL-7R α expression depends on NOTCH1 signaling (29–31). These signals are very strong in thymocytes from DN1 through the DN3a stages, decreasing abruptly during the transition to the DN3b thymocyte stage and in DP thymocytes due to

inhibited NOTCH1 expression and subsequent reduction in IL-7R α expression as a consequence of pre-TCR signaling (10, 28, 32).

Previous experiments with DN3a thymocytes demonstrated that the activity of E γ and E δ measured by their ability to activate *Tcrg* and *Tcrd* germline transcription is induced by NOTCH1-dependent recruitment of RUNX1 and MYB (14, 16, 33–37); these factors are dissociated in DP thymocytes because of pre-TCR signaling-dependent inhibition of *Notch1* expression, indicating a molecular mechanism of *Tcrg* and *Tcrd* silencing during thymocyte development (14). Hence, NOTCH1 plays an important role in enhancer-dependent *Tcrg* and *Tcrd* germline transcription and TCR $\gamma\delta$ expression during thymocyte development and thus in the generation of $\gamma\delta$ T cells. Interestingly, IL-7R signaling is required for *Tcrg* germline transcription and V γ J γ rearrangement (38–43), explaining the absence of $\gamma\delta$ T lymphocytes in *Il7ra*^{-/-} and *Il7*^{-/-} mice. IL-7R-dependent recruitment of STAT5 to *Tcrg* enhancers and promoters is essential for activating the noncoding germline transcription that triggers V γ J γ recombination (16, 44–47). STAT5 binding to E γ is lost in DP thymocytes because IL-7R signaling is terminated, constituting an additional mechanism of *Tcrg* silencing (16). In mature T cells, IL-7R signaling is also necessary for transcription of the rearranged *Tcrg* (48).

Hence, both IL-7R-dependent STAT5 and NOTCH1-dependent RUNX1 and MYB dissociation from E γ cause *Tcrg* silencing in DP thymocytes (14, 16). Based on the parallel regulation of E γ and E δ by the NOTCH1/RUNX1 and MYB pathways in the regulation of *Tcrg* and *Tcrd* germline transcription during thymocyte development (14), we hypothesize that E δ also depends on the IL-7R/STAT5 pathway in DN3a thymocytes, similar to E γ . Our results demonstrate that IL-7R/STAT5 signaling is crucial for E δ -dependent *Tcrd* germline transcription. These data indicate that E δ and E γ are identically regulated through the same signaling pathways mediated by NOTCH1/RUNX1 and MYB and IL-7R/STAT5 in DN3a thymocytes, revealing indistinguishable mechanisms for expressing and silencing enhancer-dependent *Tcrg* and *Tcrd* germline transcripts during thymocyte development.

Materials and methods

Mice

Rag2^{-/-} and *Il7ra*^{-/-} mice have been described previously (27, 49). Three- to eight-week-old *Rag2*^{-/-} and *Rag2*^{-/-} x *Il7ra*^{-/-} mice were used in this study. The animals were housed under pathogen-free conditions in the Animal Experimentation Unit at the IPBLN-CSIC in Granada, Spain, or the Institute for Frontier Life and Medical Sciences Resources in Kyoto, Japan. All animal work followed protocols approved by the CSIC and Andalusia Government

Ethical Committees or the Kyoto University Animal Care and Use Committee.

Cells and *in vitro* stimulations, inhibitions and viral transduction

SCID.adh cells have been previously described (50). The cells used in this study were from the original parental cells, which are mostly committed to the T-cell lineage (51, 52). They were cultured in RPMI 1640 medium with 10% fetal calf serum, sodium pyruvate, nonessential amino acids, glutamine, penicillin/streptomycin, and 50 μ M 2-mercaptoethanol. Jurkat-green fluorescent protein (GFP)- and Jurkat-IL7R α -GFP-expressing cells have been previously described (53). These cells were cultured in RPMI 1640 medium with 10% fetal calf serum, glutamine, and penicillin/streptomycin. SCID.adh cells (1×10^5 cells/mL) and Jurkat-GFP and Jurkat-IL7R α -GFP cells (5×10^5 cells/mL) were stimulated in culture with 10 ng/mL murine recombinant IL-7 (Peprotech) for 30 minutes to 48 hours, as indicated. SCID.adh cells (1×10^5 cells/mL) were incubated with 20 ng/mL phorbol acetate myristate and 0.5 μ g/mL ionomycin (Sigma–Aldrich, Merck) or 16 μ M γ -secretase inhibitor 7(B-(3,5-difluorophenyl)-1-alanyl)-s-phenyl-glycine t-butyl ester) (DAPT) (Selleckchem) for 24 hours. Viral transduction of SCID.adh cells with MigR retroviral plasmids was previously described (14, 54).

Quantitative reverse transcription polymerase chain reaction

To analyze transcription in SCID.adh cells, total RNA was obtained with peqGOLD TriFast (Peqlab) or Trifast (VWR). For RT–qPCR and the analysis of enhancer RNA (eRNA) transcripts in SCID.adh cells, genomic DNA-free RNA was obtained using Nucleospin plus columns (Macherey Nagel), and contaminating genomic DNA was eliminated by treatment with RNase-free DNaseI (2270A, Takara) in the presence of an RNase inhibitor (2313A, Takara) for 1 hour at 37°C, followed by two consecutive phenol/chloroform extraction steps (Amresco/Merck). The DNase I treatment and extraction steps were repeated, and RNA was ultimately precipitated by adding ethanol to a final concentration of 70% with RNase-free glycogen as the carrier. The presence of genomic DNA contamination was determined by quantitative PCR (qPCR) using the E γ 4 primers used in quantitative chromatin immunoprecipitation (qChIP) experiments. cDNA was obtained from 500 ng of total RNA with PrimeScript RT master mix (RR036, Takara) and dissolved in 100 μ L with Milli-Q water. qPCRs were performed in 96-well plates (VWR) with 4 μ L of cDNA in 10- μ L reactions prepared in duplicate using TB Green Premix Ex Taq II (RR820, Takara) on a Bio-

Rad CFX-96 System. The qPCR conditions were 95°C for 7 minutes, 40 cycles of 95°C for 30 seconds, 59.5°C for 45 seconds, and 72°C for 30 seconds, followed by incubation at 95°C for 1 minute. To analyze transcription in mouse thymocytes, qPCR was performed in 96-well plates using 1 μ L of cDNA and 0.24 μ L of 50 X ROX in 12 μ L reactions in duplicate using TB Green Premix Ex Taq II (RR820, Takara) on a StepOnePlus qPCR machine (Applied Biosystems). The qPCR conditions were 40 cycles of 95°C for 30 seconds and 59.5°C for 30 seconds, followed by incubation at 95°C for 1 minute. Melting curve analyses were performed with 55°C–90°C ramping in 0.5°C steps and 5-second increments to confirm a single amplicon for each sample and primer pair analyzed. The expression of individual genes was calculated using the Δ Ct method and normalized to *Actb* transcription. All RT–qPCR experiments were performed with at least three biological replicates. The primers for *Actb*, *ACTB*, *C γ* and *C δ* transcripts have been previously described (14). The primers were obtained from Metabion and Integrated DNA Technologies, and their sequences are listed in Table S1. Primer sequences for eRNA detection are shown in Table S1 and Figure S2.

Analyses of assays for transposase-accessible chromatin using sequencing (ATAC-seq), chromatin immunoprecipitation using sequencing (ChIP-seq), and transcriptome (RNA-seq) databases

Guidelines for the design of primers for detection of eRNAs based on factor binding detection by ChIP-seq were previously described (55). To design the primers to detect eRNAs, we focused our search on the 250–500 bp sequences flanking the 324-bp mouse E δ fragment, based on its homology with the equivalent human E δ fragment, and the 227-bp mouse E γ 4 fragment, where functional transcription factors are known to bind (44, 56) (Figures S2, S3). To confirm that the designed primers are specific for detecting E δ and E γ 4 transcripts, we analyzed chromatin profiles, transcript annotation, candidate *cis*-regulatory elements (cCREs), factor binding by ChIP-seq and RNA-seq in a 2.6-kb E δ region and a 2.8-kb E γ 4 region using available databases (Figures S2, S4–S6). ATAC-seq data in DN2b and DN3 thymocytes and $\gamma\delta$ T lymphocytes were retrieved from the Immunological Genome Project databrowsers (www.immgen.org) (57). Transcript annotation from GENCODE and the National Center for Biotechnology Information, cCREs from the ENCODE Registry, and transcription factor ChIP-seq information from ReMap Atlas of Regulatory Regions were retrieved using the UCSC Genome Browser. The ENCODE Registry of cCREs includes DNaseI hypersensitive sites across ENCODE samples that are supported by eH3K4me3, H3K27ac

or CTCF binding by ChIP-seq. RNA-seq and H3K27ac ChIP-seq analyses in DN thymocytes were obtained from data series GSE80272 (58) and analyzed using Integrative Genomic Viewer (<https://igv.org>) (Figure S6).

Electrophoretic mobility shift assays

For use in EMSAs, SCID.adh cell extracts were obtained from 10^7 unstimulated and mouse recombinant IL-7-stimulated cells for 30 minutes at 37°C. After washing with Hank's balanced salt solution (Cultek), cells were resuspended in 200 mM NaCl, 50 mM Tris-HCl (pH: 8.0), 0.75 mM spermidine, 0.15 mM spermine, 0.1 mM EDTA, 0.1 mM Na_3VO_4 , 1 mM DTT, 0.5 mM PMSF, and 1X complete protease inhibitors (Roche, Merck), lysed by adding Nonidet-40 to a 10% solution to a final concentration of 0.4% and incubated for 30 minutes on ice. Lysates were clarified by centrifugation at $12,000 \times g$ for 10 minutes at 4°C, and glycerol was added to a final proportion of 25%. The protein concentration was determined by the Bradford assay (Bio-Rad). A total of 60,000 cpm of ^{32}P -labeled double-stranded oligonucleotide was incubated with 12 μg of cell extract in a 25- μL volume containing 10 mM Tris-HCl (pH 7.5), 50 mM NaCl, 1 mM EDTA, 2% glycerol, 1 μg of poly(dI-dC), and 1 μg of bovine serum albumin for 20 minutes on ice. One microgram of anti-STAT5 antibody (Santa Cruz Biotechnology, sc-835), which recognizes STAT5a and STAT5b, was added and incubated for 30 minutes at room temperature to supershift the specific complex. The binding sites are listed in Table S1. Native polyacrylamide (4.5%) containing bis-acrylamide/acrylamide (1:19) containing 0.25X Tris-borate-EDTA previously run at 200 V for 1 hour was used to separate the DNA and DNA/protein complexes. The gels were fixed with 30% methanol and 10% acetic acid for 30 minutes and then dried and exposed to film. The primers of the tested binding sites were obtained from Metabion, and the sequences are listed in Table S1.

Quantitative chromatin immunoprecipitation

qChIP experiments were performed with chromatin from 10^7 cells incubated with 5 μg of anti-STAT5 (Santa Cruz Biotechnology, sc-235), trimethylated lysine 4 of histone H3 (H3K4me3) (ab8580, Abcam), acetylated lysine 27 of histone H3 (H3K27ac) (ab4779, Abcam), or control (clone 1-1, Millipore, Merck or ab46540, Abcam) antibodies as previously described (14). The primers used for E γ , E δ , the *Tcra* enhancer (E α), and *Oct2* exon in the qChIP have been previously described (14, 59). The primers were obtained from Metabion, and the sequences are listed in Table S1.

Luciferase assays

Reporter plasmids containing the firefly luciferase reporter gene driven only by a human TRDV1 promoter (V δ 1p) alone and a human 370-bp E δ fragment driven by V δ 1p were constructed based on the pXPG plasmid as previously described (60). Reporter plasmids containing the firefly luciferase reporter gene driven only by a minimal murine *Fos* promoter (cfosp) and by cfosp with murine 410-bp E γ 1 were constructed based on the pGL4.10 plasmid (Promega) as previously described (14, 44). To introduce a point mutation in the STAT5-binding site present in the $\delta\text{E}6/7$ region ($\delta\text{E}6/7$) of the E δ 370-V δ 1p-luciferase plasmid, a Q5 site-directed mutagenesis kit (E0554, New England Biolabs) was used with HPLC purified primers designed by the NEBaseChanger program. The sequences of the primers used are listed in Table S1. The mutation was confirmed by DraI digestion and sequencing. For luciferase assays, 5×10^6 Jurkat-GFP or Jurkat-IL7R α cells were transfected by electroporation with 5 μg of the firefly luciferase reporter plasmid and 10 ng of the pRL-TK (Promega) Renilla luciferase reporter plasmid. Both electroporation and measurements of firefly and Renilla luciferase activities were performed as previously described (14).

Statistical analysis

Statistical analysis was performed with Prism 5.0 software (GraphPad). At least three independent experiments were performed in all cases. The number of independent experiments analyzed (n) is indicated in the figure legends. Nonparametric unpaired Student's t tests with the Welch correction were performed, and significant differences between the indicated values are indicated by asterisks as follows: $p < 0.05$ (*), $p < 0.005$ (**), and $p < 0.0005$ (***). The absence of an asterisk indicates that the change relative to the control was not statistically significant.

Results

IL-7R signaling activates *Tcrd* germline transcription in DN3a thymocytes

Tcrd is flanked by *Tcra* V α and J α gene segments and comprises V δ gene segments interspaced with V α segments within an ~1 Mb region, followed by a 33.7-kb region that contains two D δ (Trdd1 and Trdd2) gene segments, two J δ (Trdj1 and Trdj2) gene segments, E δ , the *Tcrd* C region (C δ), and the inverted Trdv5 gene segment in murine chromosome 14 (9) (Figure S1). *Tcrg* spans 0.2 Mb and comprises three functional V γ -J γ -*Tcrg* C region (C γ 1, C γ 2 or C γ 4)-E γ clusters

in murine chromosome 13 (9) (Figure S1). Expression of the TCR γ and TCR δ chains results from the activation of enhancer-dependent germline transcription of their respective unrearranged genes, which induces long-range chromatin changes that trigger V γ J γ and V δ D δ J δ recombination in DN2b and DN3a thymocytes (Figure S1). These noncoding transcripts are initiated by promoters associated with the J γ , D δ , and J δ gene segments that are ultimately spliced into their respective constant regions (40, 61) (Figure 1). The levels of germline transcription measured at these constant regions represent the

sum of all the transcripts that are initiated in the D and/or J gene segments in their respective gene or gene cluster. To evaluate the potential role played by IL-7R signaling in the activation of *Tcrd* germline transcription, cells of the appropriate developmental stage that are deficient in V(D)J recombination must be used. We analyzed the levels of C δ transcripts in untreated and IL-7-treated SCID.adh cells and compared them with the well-known regulation of *Tcrg* germline transcription by measuring IL-7-dependent activation of C γ transcripts (40, 41) (Figure 2A). These cells, which were derived from mice carrying an

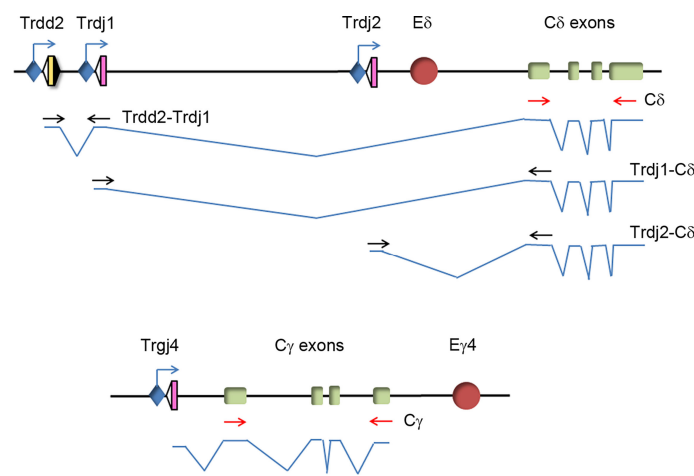


FIGURE 1
Structure of *Tcrd* and *Tcrg* germline transcripts. Transcription and splicing are indicated by blue lines. The position of primers used to detect specific germline transcripts is indicated: primers used to detect C δ and C γ transcripts are represented in red, and primers to detect Trdd2-Trdj1, Trdj1-C δ and Trdj2-C δ transcripts are represented in black.

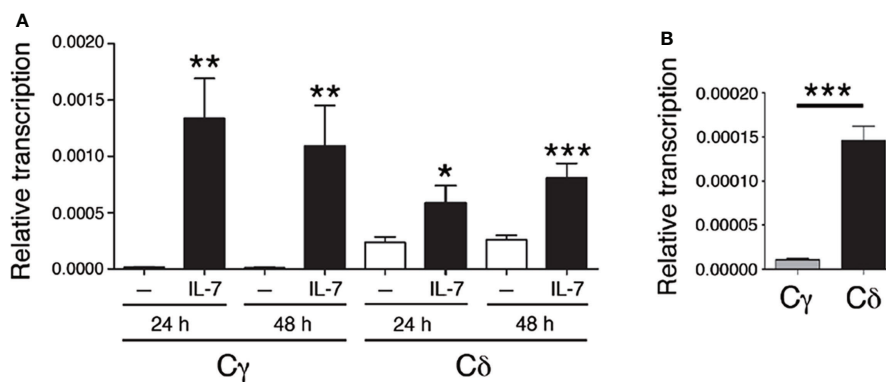


FIGURE 2
IL-7 activates *Tcrg* and *Tcrd* germline transcription. (A) Analysis of C γ and C δ transcription in untreated (-, white bars) and IL-7-treated SCID.adh cells (IL-7, black bars) after 24 or 48 hours, as indicated, as determined by RT-qPCR. (B) Transcriptional analysis of C γ and C δ in untreated SCID.adh cells cultured for 24 hours, as determined by RT-qPCR. The results were normalized to those of *Actb* and represent the mean \pm standard error of the mean (SEM) of duplicate RT-qPCRs based on 8 independent experiments. Nonparametric unpaired Student's t tests with the Welch correction were performed, and *p* values are represented by asterisks as follows: *p* < 0.05 (*), *p* < 0.005 (**), and *p* < 0.0005 (***). The significance of the difference between values obtained with untreated and IL-7-treated cells is shown.

inactivating spontaneous point mutation in the catalytic subunit of DNA-PK, exhibit a DN3a-like phenotype derived from their complete defect in V(D)J recombination (50, 62). Because their TCR genes are in a germline unrearranged configuration, these cells constitute an excellent model with which to study IL-7R-dependent *Tcrg* transcription, as well as pre-TCR-induced silencing of *Tcrg* and *Tcrd* and activation of *Tcrα* (14, 16, 44, 45, 60, 63). Due to a deletion at the 5'-end of the *Tcrg* locus in these cells, germline transcription of C γ 4 (C γ) was analyzed as representative of the three V γ -J γ -C γ clusters because they share the same regulation (16) (Figure 1). Although basal C δ transcription was found to be higher than C γ transcription in these cells, IL-7 treatment clearly induced both C γ and C δ transcription (Figures 2A, B).

IL-7R-dependent activation of *Tcrg* and *Tcrd* germline transcription is regulated by Notch signaling

Regulation of enhancer-dependent *Tcrg* and *Tcrd* germline transcription is regulated by Notch signaling (14). Because IL-

7R α is a target of Notch signaling (14, 29–31), we evaluated the effect of gain and loss of NOTCH1 signaling on *Il7ra*- and IL-7-dependent C γ and C δ transcription (Figure 3). As expected (14), transduction of SCID.adh cells with intracellular NOTCH1 domain (ICN1)-expressing retroviruses induced *Il7ra* transcription (Figure 3A). Accordingly, IL-7-dependent activation of C γ and C δ transcription was induced in SCID.adh cells that had been transduced with ICN1 + GFP-expressing retroviruses, and the transcription levels were compared with those of cells that had been transduced with retroviruses that expressed only GFP (Figures 3B, C). In contrast, cell treatment with the γ -secretase inhibitor DAPT, which inhibits proteolytic cleavage and thus prevents the release of endogenous ICN1, inhibited *Il7ra* transcription (Figure 3D); therefore, a decrease in IL-7-dependent activation of C γ and C δ transcription was detected (Figures 3E, F). These results indicate that the Notch-dependent effect on *Il7ra* transcription causes increased activation of IL-7-dependent *Tcrd* and *Tcrg* germline transcription. These results confirm that the transcriptional regulatory axis formed by the NOTCH1 and IL-7R pathways was evident in SCID.adh cells and involved in the regulation of *Tcrg* and *Tcrd* transcription in DN3a thymocytes. Therefore, the

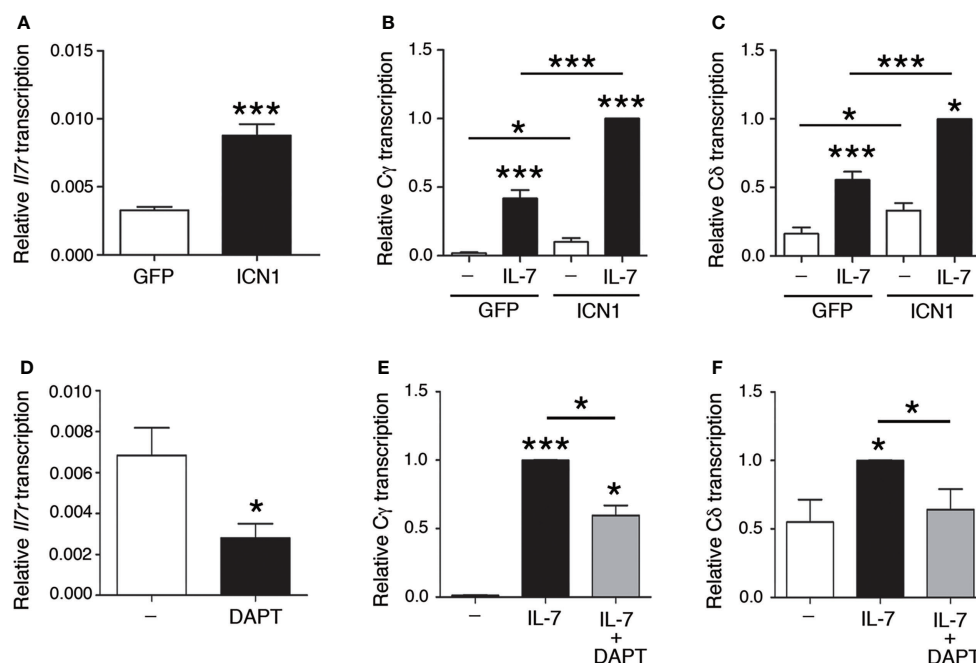


FIGURE 3

Notch-dependent regulation of IL-7R-dependent *Tcrg* and *Tcrd* germline transcription. RT-qPCR analysis of (A) *Il7ra*, (B) C γ , and (C) C δ transcription ($n=8$, $n=3$, and $n=3$, respectively) in SCID.adh cells transduced with GFP (GFP) or ICN1 + GFP (ICN1) retroviruses and incubated in the absence (-) or presence of IL-7 (IL-7), as indicated. RT-qPCR analysis of (D) *Il7ra*, (E) C γ , and (F) C δ transcription ($n=3$) in untreated or DAPT-treated SCID.adh cells incubated in the absence (-) or presence (IL-7) of IL-7, as indicated. The results were normalized to those of *Actb* and represent the mean \pm SEM of duplicate RT-qPCRs in the indicated number (n) of independent experiments. Nonparametric unpaired Student's t tests with the Welch correction were performed, and p values are represented by asterisks as follows: $p < 0.05$ (*) and $p < 0.0005$ (***). Significant differences between the obtained values in cells untreated or treated with IL-7, transduced with GFP or ICN1 + GFP retroviruses or untreated and DAPT-treated cells as indicated are shown.

mechanism for the regulation of *Tcrg* and *Tcrd* germline transcription by this regulatory axis is based on the regulation of IL-7R expression by Notch signaling, which results in increased responsiveness of the unrearranged *Tcrg* and *Tcrd* genes to IL-7.

IL-7R signaling is essential for *Tcrd* germline transcription *in vivo*

To study TCR germline transcription, thymocytes of the appropriate developmental stage (such as DN3a in the case of *Tcrg* and *Tcrd*) that are deficient in V(D)J recombination must be analyzed. *Rag2*^{-/-} mice show deficient V(D)J recombination; therefore, thymocyte development is blocked at the DN3a stage in these mice (21, 49, 64). In fact, these animals constitute a pure source of DN3a thymocytes, 99.0 ± 0.8% of total thymocytes (64). The *Tcrg* and *Tcrd* in an unrearranged configuration in these mice allowed us to analyze germline transcription in DN3a thymocytes. To clearly determine the role played by IL-7R signaling *in vivo*, we compared C γ and C δ germline transcription in *Rag2*^{-/-} and *Rag2*^{-/-} *Il7ra*^{-/-} DN3a thymocytes by performing RT-qPCR (Figure 4A). Because *Rag2*^{-/-} thymocyte blockade occurs earlier during development and predominates over *Il7ra* deficiency (28, 49), both *Rag2*^{-/-} and *Rag2*^{-/-}*Il7ra*^{-/-} mice have an equivalent block at the DN3a stage.

As expected (40), C γ transcription was abrogated in *Rag2*^{-/-} *Il7ra*^{-/-} DN3a thymocytes. Our analyses of C δ transcription indicated that *Tcrd* germline transcription was also strongly dependent on IL-7R signaling (Figure 4A). C δ transcripts constitute the sum of *Tcrd* germline transcripts initiated at the *Trdd2*, *Trdj1*, and *Trdj2* promoters (Figure 1). We also analyzed specific transcripts initiated at each of these promoters. The transcripts initiated at the *Trdj1* and *Trdj2* promoters are spliced to the first exon of C δ , while those initiated at the *Trdd2* promoter are first spliced to the *Trdj1* gene segment before splicing to the C δ first exon (Figure 1). The *Trdd2*-*Trdj1*, *Trdj1*-C δ and *Trdj2*-C δ transcripts were clearly detected in *Rag2*^{-/-} thymocytes (Figure 4B). According to the strong inhibition of C δ transcription, the aforementioned transcripts were profoundly inhibited in *Rag2*^{-/-} *Il7ra*^{-/-} thymocytes (Figure 4B). These results indicate that, similar to *Tcrg* germline transcription, *Tcrd* germline transcription depends on IL-7R signaling in DN3a thymocytes.

STAT5 binds to E δ

IL-7R signaling results in rapid phosphorylation of STAT5, which is translocated from the cytoplasm to the nucleus to activate its target genes. Accordingly, IL-7R signaling activates C γ transcription through the recruitment of STAT5 to E γ (44).

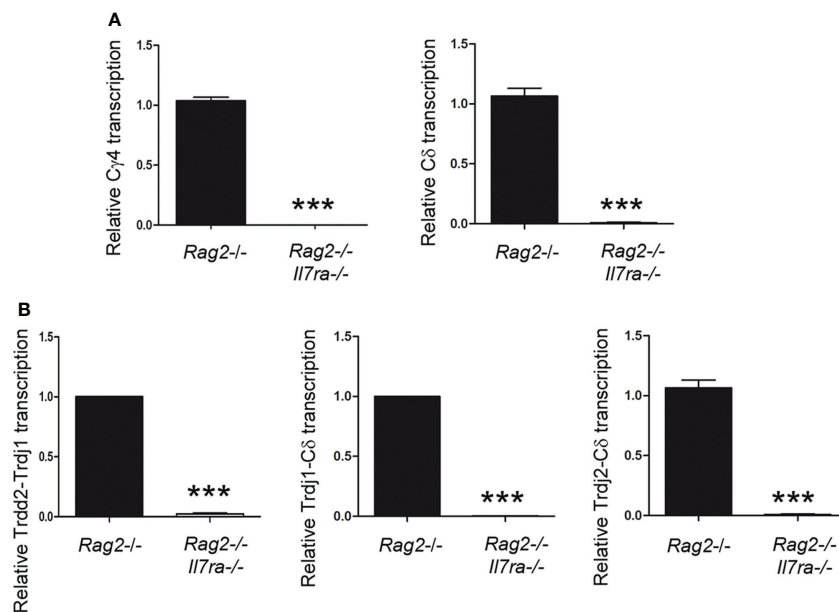


FIGURE 4

IL-7R signaling is essential for *Tcrd* germline transcription *in vivo*. Analysis of (A) C γ and C δ and (B) *Trdd2*-*Trdj1*, *Trdj1*-C δ and *Trdj2*-C δ transcripts in *Rag2*^{-/-} and *Rag2*^{-/-} *Il7ra*^{-/-} thymocytes by RT-qPCR. The results were normalized to those of *Actb* and represent the mean ± SEM of duplicate RT-qPCRs based on 3 independent experiments. Nonparametric unpaired Student's *t* tests with the Welch correction were performed, and *p* < 0.0005 values based on values obtained with *Rag2*^{-/-} and *Rag2*^{-/-} *Il7ra*^{-/-} thymocytes are represented by asterisks as *** (*p* < 0.0005).

We compared STAT5 binding to E γ 4 and E δ by qChIP in unstimulated and IL-7-stimulated SCID.adh cells after a 30-minute treatment (Figure 5A). We found comparable STAT5 recruitment to both E γ 4 and E δ upon IL-7 treatment. To confirm the recruitment of STAT5 in primary DN3a cells, we evaluated its binding in *Rag2*^{-/-} thymocytes (Figure 5B). IL-7 treatment was not necessary to detect STAT5 binding to these enhancers in ex-vivo *Rag2*^{-/-} thymocytes, most likely because these cells were already stimulated *in vivo*. We found similar STAT5 binding to both enhancers, confirming the results obtained with SCID.adh cells. As a negative control in our qChIP experiments, STAT5 binding to an *Oct2* exon sequence was also analyzed (Figures 5A, B).

IL-7R signaling activates E δ function through STAT5 binding to the δ E6/7 site

eRNAs together with epigenetic activation marks on histone H3, such as trimethylation of lysine 4 (H3K4me3) and acetylation of lysine 27 (H3K27ac) are predictors of enhancer activity (65–68). To evaluate whether IL-7 treatment can directly activate E δ and E γ activity, we analyzed the effect of IL-7R signaling on H3K4me3 and H3K27ac on E δ and E γ 4 in unstimulated and IL-7-treated SCID.adh cells (Figures 6A, B). Consistent with the presence of these chromatin marks on active enhancers (67, 68), we found that H3K4me3 and H3K27ac modification was strongly induced at both enhancers, but not

at a negative control sequence, after IL-7 stimulation of SCID.adh cells. Detection of eRNAs is the most reliable indicator of enhancer activity (65, 66). These noncoding transcripts are unidirectional or bidirectional and have low abundance due to their instability. Enhancer activation correlated with IL-7-dependent induction of bidirectional E δ and E γ 4 eRNAs in SCID.adh cells (Figures 6C, D). To examine the presence of other *cis*-regulatory regions in the surrounding enhancer regions, we analyzed chromatin accessibility in DN2b and DN3 thymocytes, and $\gamma\delta$ T lymphocytes by ATAC-seq using the Immunological Genome Project databrowsers (www.immgen.org) (57), as well as the presence of other enhancers in the vicinity according to the ENCODE Registry of cCREs (Figures S2, S4, S5). Although these analyses indicate the presence of other *cis*-regulatory elements located in the vicinity of E δ and E γ 4 within a region of less than 2 kb, these enhancers constitute the sequences with the highest density of transcription factor binding by ChIP-seq according to ReMap Atlas of regulatory regions (Figures S4, S5). Interestingly, p300 and STAT5 are specifically recruited to these enhancers (Figures S4, S5). Taken together, these data clearly demonstrate that E γ and E δ are both activated by IL-7R signaling.

To directly evaluate the role of IL-7 on E δ function, we analyzed its effect on enhancer activity using luciferase reporter constructs in transiently transfected Jurkat cells (Figure 7). These cells constitute a well-established model for studying TCR enhancer activity upon cell stimulation (14, 60). Because these cells express very low levels of IL7R α , we used two Jurkat clones

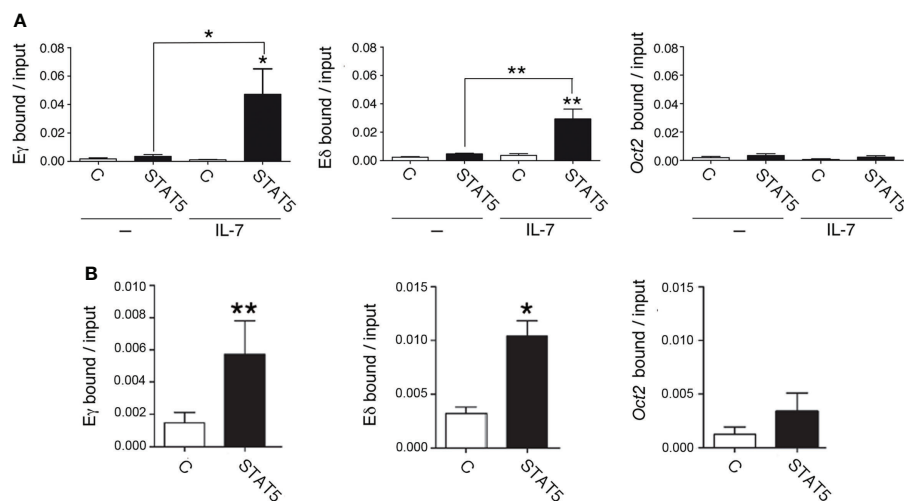


FIGURE 5

IL-7R signaling induces STAT5 recruitment to E γ and E δ in DN3a thymocytes. (A) Binding of STAT5 to E δ , E γ 4 and *Oct2* sequences in untreated (-) and IL-7-treated (IL-7) SCID.adh cells determined after 30 minutes by qChIP (n=8). (B) Binding of STAT5 to E δ , E γ 4 and *Oct2* sequences in *Rag2*^{-/-} thymocytes as determined by qChIP (n=4). The data represent the mean \pm SEM of duplicate results obtained from n independent qChIP experiments. Nonparametric unpaired Student's t tests with the Welch correction were performed as indicated, and p values are represented by asterisks as follows: $p < 0.05$ (*) and $p < 0.005$ (**). Significance between the values obtained using an anti-STAT5 antibody (STAT5) and control antibody (C), as indicated, is shown.

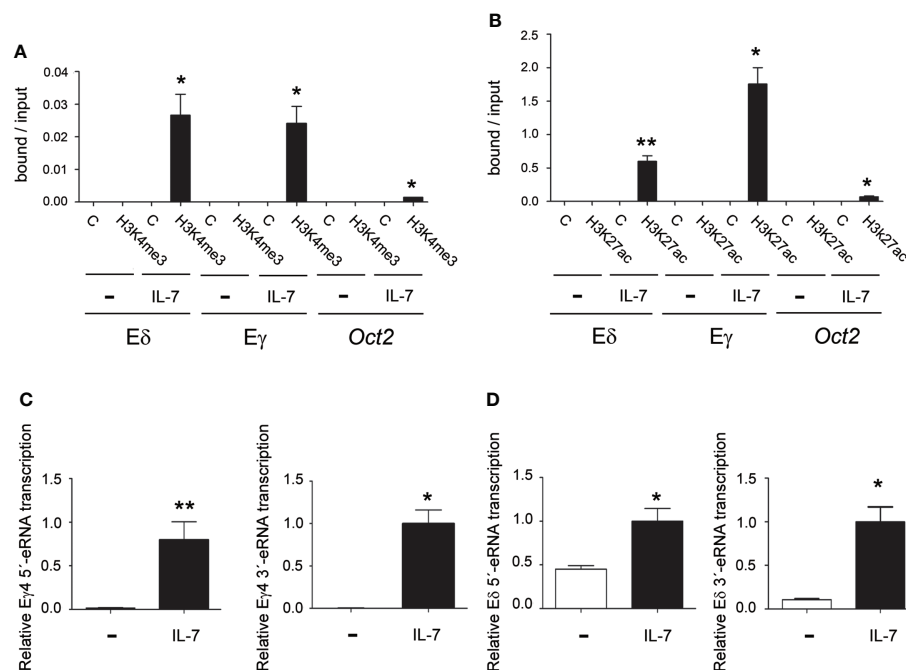


FIGURE 6

IL-7R signaling activates E γ and E δ epigenetic marks and eRNA transcription. Analyses of H3K4me3 (A) and H3K27ac (B) histone marks in E γ , E δ and Oct2 sequences in untreated (-) and IL-7-treated (IL-7) SCID.adh cells as determined after 24 hours by qChIP. The data represent the mean \pm SEM of duplicate results obtained from 4 independent qChIP experiments. Nonparametric unpaired Student's t tests with the Welch correction were performed as indicated, and the significance of differences between the values obtained using anti-H3K4me3 or anti-H3K27ac and control antibodies (C) are shown. Analyses of E γ (C) and E δ (D) eRNA transcription in untreated (-) and IL-7-treated (IL-7) SCID.adh cells after 24 hours by RT-qPCR. The results were normalized to those of *Actb* and represent the mean \pm SEM of duplicate RT-qPCRs from 3 independent experiments. Nonparametric unpaired Student's t tests with the Welch correction were performed, and the significance of differences between the values obtained with untreated and IL-7-treated cells is shown. *p* values are represented by asterisks as follows: *p*<0.05 (*) and *p*<0.005 (**).

that had been previously obtained through retroviral transduction and that expressed GFP or IL7R α + GFP (53). As shown in Figure 7A, the GFP-expressing cells exhibited very low levels of *IL7RA* expression compared with the cells transduced with GFP + IL7R α -expressing retroviruses. As expected, E γ activity was highly activated by IL-7 treatment in the IL7R α + GFP-expressing cells but not in the control GFP-expressing cells (Figure 7B). Similarly, we found that E δ activity was activated by IL-7 only in the IL7R α + GFP-expressing cells and not in the control GFP-expressing cells (Figure 7B). The observed effects were clearly mediated by the respective enhancer because the luciferase activity of the constructs with no enhancer in either clone was unaffected by IL-7 treatment. Of the two conserved putative STAT5 sites found by comparing murine and human E δ sequences (Figure S3), we validated by EMSA the STAT5-binding site that was located between δ E6 and δ E7, the δ E6/7 site (Figures S7A, B). STAT5 binding to this site is consistent with recruitment data for this factor to E δ by ChIP-seq in immune cells and tissues based on ReMap Atlas of Regulatory Regions (Figure S4). Introduction of a mutation that abolished STAT5 binding to the human δ E6/7 site (Figure S7C) abrogated

enhancer activation by IL-7 treatment in IL7R α -expressing transfected Jurkat cells (Figure 7B). Together, our results demonstrate that, in addition to the regulation of *Tcr* germline transcription and E γ function, IL-7R signaling is crucial for E δ -dependent *Tcrd* germline transcription.

Discussion

E γ and E δ are regulated in parallel during β -selection, activating germline transcription and V γ J γ and V δ D δ J δ recombination in DN2b and DN3a thymocytes and gene silencing in DP thymocytes (15, 69). Pre-TCR signaling causes dissociation of E γ - and E δ -bound factors in DP thymocytes (14–16). MYB and RUNX1 dissociate from E γ and E δ during β -selection as a result of the pre-TCR-dependent downregulation of *Notch1* transcription (14, 32), whereas STAT5 dissociates from E γ as a result of terminated *Il7ra* transcription (16). In this study, we demonstrate that E δ function depends on IL-7R-dependent STAT5 recruitment, similar to the mechanism of E γ function induction, demonstrating a parallel regulatory

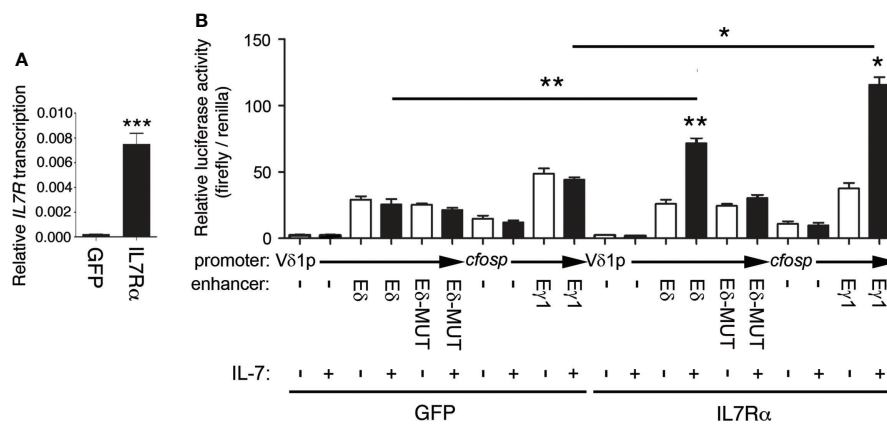


FIGURE 7

Eδ is activated by IL-7R signaling. **(A)** Transcriptional analysis of IL7R in GFP- (GFP) and IL7Rα-GFP- (IL7Rα)-expressing Jurkat cells. The results were normalized to those of *ACTB* and represent the mean \pm SEM of duplicate RT-qPCRs based on 3 independent experiments. The significance of differences between the values obtained with GFP- and IL7Rα-GFP-expressing Jurkat cells is shown. **(B)** Transcriptional analysis of Eδ-, Eδ-MUT- and Eγ1-dependent luciferase constructs transfected into GFP- (GFP)- or IL7Rα-GFP- (IL7Rα)-expressing Jurkat cells that were untreated (-) or treated with IL-7 (+) for 48 hours. The data represent the mean \pm SEM of duplicate results obtained from 6 independent firefly/Renilla luciferase assays. The significance of differences between the values obtained from untreated and IL-7-treated cells, as indicated, is shown. Nonparametric unpaired Student's *t* tests with the Welch correction were performed, and *p* values are represented by asterisks as follows: *p* < 0.05 (*), *p* < 0.005 (**), *p* < 0.0005 (***).

mechanism of these enhancer functions in controlling *Tcrγ* and *Tcrδ* germline transcription. Hence, the activity of *Eγ* and *Eδ* depends on RUNX1, MYB, and STAT5 recruitment in DN3a thymocytes, whereas these three aforementioned factors dissociate from *Eγ* and *Eδ* in DP thymocytes as a consequence of termination of Notch and IL-7R signaling, revealing the molecular mechanism by which *Tcrγ* and *Tcrδ* transcription is regulated in parallel during thymocyte development.

To study the role of the combined effect of IL-7 and Notch signaling, we analyzed the effect of IL-7 on ICN1-transduced SCID.adh cells. These cells produce full-length and truncated *Notch1* transcripts, which derive from an intragenic deletion of approximately 38 kb and consist of exon 1 joined to an 81-kb noncontiguous intron 1 sequence that is spliced to a site 12 bp 3' of the exon 28 splice acceptor site (70). The resulting polypeptide can insert into the cell membrane due to its hydrophobic N-terminus, driving ICN1 expression to generate ligand-independent signals in a DAPT-sensitive fashion. Previous studies have demonstrated that SCID.adh cells constitutively express some levels of ICN1 and respond to DAPT by downregulating ICN1 expression as well as Notch-dependent genes, such as *Cd25*, *Hes1*, *Il7ra*, *Runx1*, *Tcrδ* and *Tcrγ* (14, 70, 71). In addition, these cells respond to IL-7 signaling and have been previously used to analyze its role in regulating *Tcrγ* germline transcription (14, 44, 45). Therefore, SCID.adh cells constitute an excellent model to study the combined effect of Notch and IL-7 in the regulation of *Tcrγ* and *Tcrδ* germline transcription. Consistent with the induction of *Il7ra* transcription by Notch, our results revealed that IL-7-dependent activation of *Tcrδ* and *Tcrγ* germline

transcription was further activated by ICN1 and inhibited by DAPT in these cells. These results strongly suggest that the Notch-dependent effect on *Il7ra* transcription is responsible for the IL-7-dependent *Tcrδ* and *Tcrγ* germline transcription observed upon ICN1 overexpression and DAPT treatment in SCID.adh cells.

To demonstrate the essential role for IL-7 signaling in activating *Eδ* and *Eγ4* in SCID.adh cells, we analyzed H3K4me3 and H3K27ac together with the induction of eRNAs as predictors of enhancer activity (65–68). In fact, enhancer transcription is considered the best indicator of enhancer activity (65, 66). The detection of IL-7-induced *Eγ* and *Eδ* transcripts indicates that this treatment induces an opening in the chromatin structure at the enhancer regions. Although other open regions that could function as *cis*- regulatory elements are present in the vicinity of *Eδ* and *Eγ4*, as indicated by ATAC-seq and the ENCODE Registry of cCREs, these enhancers concentrate the highest binding density of transcription factors, including the specific binding of p300 and STAT5 (Figures S2, S4, S5). This high density of transcription factors that bind to *Eδ* and *Eγ4* is consistent with the absence of H3K27ac at the core site of these enhancers, with this histone mark detected in the flanking regions of these enhancers (Figures S4–S6). These analyses confirm that *Eδ* and *Eγ4* are the main regulatory elements present in the regions analyzed. Because STAT5 specifically binds to *Eδ* and *Eγ4* and not to other nearby enhancers as analyzed by ChIP-seq based on ReMap Atlas of Regulatory Regions, our data indicating that the measured transcripts are IL-7 responsive strongly support that they constitute true *Eδ* and *Eγ4* eRNAs. Although the distal enhancer EO581865/enhD, located adjacent to *Eδ* at a distance

of approximately 100 pb, exhibits some levels of STAT5 binding based on ReMap data, ATAC-seq experiments indicate that the EO581865/endD chromatin is not accessible in DN2b and DN3 thymocytes, indicating that E δ is the relevant enhancer at the *Tcrd* locus during thymocyte development (Figure S4). The low levels of transcripts detected in E δ and E γ 4 surrounding regions by RNA-seq in DN thymocytes are consistent with the expected low abundance of eRNAs (Figure S6). Although the role of eRNAs remains unresolved, they are thought to be relevant to maintaining an open chromatin state that is readily accessible for transcription factors, stabilizing enhancer-promoter looping interactions, promoting the loading of RNA-polymerase 2 to the promoter, and/or releasing a paused promoter to an elongating stage (72–74). Our experiments do not address the potential roles of these eRNAs on *Tcrd* and *Tcrd* transcription, but these transcripts likely contribute to maintaining the opening of enhancer chromatin to facilitate access to transcription factors and cofactors in the activation of their specific promoters.

Previous experiments with *Il7ra*^{-/-} mice demonstrated a strong dependence on IL-7R signaling in the regulation of *Tcrd* germline transcription and V δ D δ J δ recombination and little apparent effect on *Tcrd* recombination (38–42, 48). Although a partial inhibitory effect on V δ D δ J δ might be overlooked in these experiments (38), these results differ from our results, with dramatically reduced *Trdd2*, *Trdj1* and *Trdj2* germline transcription observed in *Rag2*^{-/-} *Il7ra*^{-/-} DN3a thymocytes and IL-7R-dependent regulation of E δ . Consistent with the important role played by E δ in promoting chromatin accessibility and activating *Trdd2*, *Trdj1* and *Trdj2* germline transcription in a discrete chromatin loop (75), previous experiments with E δ ^{-/-} mice demonstrated that this enhancer is important for *Tcrd* germline transcription and V δ D δ J δ rearrangements in DN3a thymocytes and the generation of $\gamma\delta$ T lymphocytes (23). Because *Tcrd* germline transcription primarily depends on E δ function (23), our results demonstrate that IL-7R signaling plays a crucial role in the control of E δ -dependent *Tcrd* germline transcription in DN3a cells. Therefore, the V δ D δ J δ rearrangements detected in *Il7ra*^{-/-} mice are most likely the consequence of a very low level of *Tcrd* germline transcription in *Rag2*^{-/-} *Il7ra*^{-/-} thymocytes; this low level of transcription may open the locus chromatin to permit accessibility of the recombinase machinery. Although profoundly reduced compared to the levels in the control mice, 10–12% thymic and 6–10% splenic $\gamma\delta$ T lymphocytes were detected in the E δ ^{-/-} mice; the presence of some $\gamma\delta$ T cells in E δ ^{-/-} mice suggested the implication of additional elements in activating V δ D δ J δ recombination. Our data indicate that nearly all *Tcrd* germline transcripts were abrogated in *Rag2*^{-/-} *Il7ra*^{-/-} thymocytes compared to *Rag2*^{-/-} thymocytes, including those initiated by the *Trdd2* promoter (Figure 4), which had been previously proposed to be a possible candidate for promoting *Tcrd* germline transcription and V δ D δ J δ recombination in E δ ^{-/-} mice (61). The detection of only residual *Tcrd* transcripts in our analysis of *Rag2*^{-/-} *Il7ra*^{-/-} thymocytes does not support a suggestion of additional IL-7R-

independent regulatory elements in the activation of V δ D δ J δ recombination. Since our experiments were focused on the regulation of *Tcrd* and *Tcrd* germline transcription that occur prior to V δ D δ J δ and V γ J γ rearrangements and thus TCR $\gamma\delta$ expression, these data do not directly address the issue of $\alpha\beta$ vs. $\gamma\delta$ T-cell commitment, which is accepted to be regulated by differential signaling strength between TCR $\gamma\delta$ and pre-TCR expressed on the same T-cell precursors (11–13).

In contrast to its important function in *Tcrd* germline transcription and V δ D δ J δ recombination in thymocytes, E δ is not required for the transcription of a rearranged *Tcrd* gene in mature $\gamma\delta$ T lymphocytes; in fact, E α is the regulatory element critical for this transcriptional function (23, 76). IL-7R signaling does not activate *Tcrd* germline transcription or induce STAT5 binding to E α in SCID.adh cells (Figures S8A, B). In contrast, IL-7R signaling has been previously shown to be involved in preventing premature V α J α recombination in DN4 thymocytes (28). Therefore, IL-7R signaling is probably not required for rearranged *Tcrd* transcription in mature $\gamma\delta$ T cells. Because E δ is critical for the premature V α J α rearrangements that have been detected in E α ^{-/-} mice that result in the detection of V α 2⁺ T lymphocytes in these mice (76–78), NOTCH1 and IL-7R signaling likely regulate the induction of E δ -dependent V α J α rearrangements in DN3a thymocytes.

Comparisons between synthetic and natural enhancers have revealed that enhancer activity is best explained by occupancy of specific binding sites regardless of the binding site position (79). Hence, the combination of multiple transcription factor-binding sites and not their organization underlies the specificity of eukaryotic gene expression regulation (80). In addition, temporal expression of specific transcription factors clearly regulates T-lineage identity and development (24). In this regard, the combination of the essential binding sites for RUNX1, MYB and STAT5 is conserved between E γ and E δ in both mice and humans; however, these sites are positioned differently from STAT5-MYB-RUNX1 sites in E γ and RUNX1-MYB-STAT5 sites in E δ (Figure S7). Therefore, the recruitment of these factors to differently organized binding sites within these enhancers could create efficient regulatory structures that are critical for high *Tcrd* and *Tcrd* gene expression in DN2b and DN3a thymocytes and gene silencing in DP thymocytes and $\alpha\beta$ T lymphocytes. We have not directly addressed the effect of IL-7 on the recruitment of RUNX1 and MYB to E δ in SCID.adh cells; however previous studies have shown that IL-7 treatment does not inhibit the recruitment of RUNX1 and MYB to E γ in these cells (44). The fact that RUNX1, MYB and STAT5 bind to E γ in IL-7-treated SCID.adh cells (44) as well as to E γ and E δ in *Rag2*^{-/-} thymocytes (14, 16) supports the hypothesis that these factors are simultaneously recruited to these enhancers in DN3a thymocytes. Furthermore, luciferase assays indicated that STAT5 binding synergistically augmented the activity of E γ activity along with RUNX1 and MYB (44), and

IL-7 treatment increased E δ activity (Figure 7), which is absolutely dependent on the presence of intact RUNX1 and MYB binding sites (33–36). Together, these results strongly suggest that these factors are simultaneously recruited to E δ and E γ to regulate enhancer function in DN3a thymocytes.

The functional interconnection of the IL-7R and NOTCH1 signaling pathways is essential for normal T-cell development. When this intersection is defective, lymphopenia can be a result, whereas excessive signaling can lead to the development of T-cell acute lymphoblastic leukemia (81). In fact, constitutive activation of *NOTCH1* signaling is the most prominent oncogenic pathway during T-cell transformation in more than 60% of all human T-cell acute lymphoblastic leukemia cases, which are mainly caused by different activating mutations (82). Interestingly, in 70% of the latter, chromosomal translocations are evident during thymocyte development as a result of illegitimate TCR gene recombination, with those involving *TCRD* predominant in approximately 67% of cases (83, 84) and E δ being an important element contributing to genomic instability (85). Our results revealing an important role played by IL-7R signaling in the regulation of E δ -dependent *Tcrd* germline transcription in DN3a thymocytes might contribute to a better understanding of the causes of this disease.

Data availability statement

The raw data supporting the conclusions of this article will be made available by the authors, without undue reservation.

Ethics statement

The animal study was reviewed and approved by Ethical Committee of Consejo Superior de Investigaciones Científicas, Spain Ethical Committee of Andalusian Government, Spain Animal Care and Use Committee of Kyoto University, Japan. Written informed consent was obtained from the owners for the participation of their animals in this study.

Author contributions

AR-C performed and analyzed the experiments. ST-I and KI provided the data shown in Figure 4. AC and AR-C performed the experiments shown in Figure S8. JL-R participated in experiments performed with the mice. CS participated in the interpretation of the results. CH-M designed the research, analyzed the results, made the figures and wrote the article. All authors contributed to the article and approved the submitted version.

Funding

This work was funded by grants from the Spanish Ministry of Science and Innovation (BFU2016-79699P and PID2021-128720NB-100), Spanish Scientific Research Council (2019AEP202), and Andalusian Government (P20_01271) to CH-M; the Spanish Ministry of Science and Competitiveness (PID2020-118859GB-100) and Andalusian Government (P20_01269) to CS; and JSPS KANENHI (19K08999) to ST-I. This research was co-funded with European Union funds. AR-C, JL-R, and CH-M are part of CSIC's Global Health Platform (PTI+ Salud Global) (SGL2103033).

Acknowledgments

We thank Nuno L. Alves (Institute for Molecular and Cell Biology, Porto, Portugal) and René A. W. van Lier (Academic Medical Center, Amsterdam, The Netherlands) for the Jurkat-GFP and Jurkat-IL7Ra + GFP clones; José Zamorano (San Pedro de Alcántara Hospital, Cáceres, Spain) for his help in STAT5 EMSAs; David L. Wiest (Fox Chase Cancer Center, Philadelphia, PA, USA) for SCID.adh cells; Jonathan C. Aster (Harvard Medical School, Cambridge, MA, USA) for the MigR-GFP and MigR-ICN1-GFP constructs; and Clara Sánchez-González for animal care.

Conflict of interest

The authors declare that the research was conducted in the absence of any commercial or financial relationships that could be construed as a potential conflict of interest.

Publisher's note

All claims expressed in this article are solely those of the authors and do not necessarily represent those of their affiliated organizations, or those of the publisher, the editors and the reviewers. Any product that may be evaluated in this article, or claim that may be made by its manufacturer, is not guaranteed or endorsed by the publisher.

Supplementary material

The Supplementary Material for this article can be found online at: <https://www.frontiersin.org/articles/10.3389/fimmu.2022.943510/full#supplementary-material>

References

- Chien Y-H, Meyer C, Bonneville M. $\gamma\delta$ T cells: first line of defense and beyond. *Annu Rev Immunol* (2014) 32:121–55. doi: 10.1146/annurev-immunol-032713-120216
- Wu Y-L, Ding Y-P, Tanaka Y, Shen L-W, Wei C-H, Minato N, et al. $\gamma\delta$ T cells and their potential for immunotherapy. *Int J Biol Sci* (2014) 10:119–35. doi: 10.7150/ijbs.7823
- Benveniste PM, Roy S, Nakatsugawa M, Chen ELY, Nguyen L, Millar DG, et al. Generation and molecular recognition of melanoma-associated antigen-specific human $\gamma\delta$ T cells. *Sci Immunol* (2018) 3:eav4036. doi: 10.1126/sciimmunol.aav4036
- Ono T, Okamoto K, Nakashima T, Nitta T, Hori S, Iwakura Y, et al. IL-17-producing $\gamma\delta$ T cells enhance bone regeneration. *Nat Commun* (2019) 7:10928. doi: 10.1038/ncomms10928
- Ribeiro M, Brigas HC, Temido-Ferreira M, Pousinha PA, Regen T, Santa C, et al. Meningeal $\gamma\delta$ T cell-derived IL-17 controls synaptic plasticity and short-term memory. *Sci Immunol* (2021) 4:eay5199. doi: 10.1126/sciimmunol.aay5199
- Johnson MD, Witherden DA, Havran WL. The role of tissue-resident $\gamma\delta$ T cells in stress surveillance and tissue maintenance. *Cells* (2020) 9:686. doi: 10.3390/cells9030686
- Hu B, Chengcheng J, Zeng X, Resch JM, Jedrychowski MP, Yang Z, et al. $\gamma\delta$ T cells and adipocyte IL-17C control fat innervation and thermogenesis. *Nat Commun* (2016) 578:610–4. doi: 10.1038/s41586-020-2028-z
- Li Y, Zhang Y, Zeng X. $\gamma\delta$ T cells participating in nervous systems: A story of jekill and Hyde. *Front Immunol* (2021) 12:656097. doi: 10.3389/fimmu.2021.656097
- Rodríguez-Caparrós A, Álvarez-Santiago J, Valle-Pastor MJ, Suñe C, López-Ros J, Hernández-Munain C. Regulation of T-cell receptor gene expression by three-dimensional locus conformation and enhancer function. *Int J Mol Sci* (2020) 21:8478. doi: 10.3390/ijms21228478
- Taghon T, Yui MA, Pant R, Diamond RA, Rothenberg EV. Developmental and molecular characterization of emerging β - and $\gamma\delta$ -selected pre-T cells in the adult mouse thymus. *Immunity* (2006) 24:53–64. doi: 10.1016/j.immuni.2005.11.012
- Haks MC, Lefebvre JM, Lauritsen JP, Carleton M, Rhodes M, Miyazaki T, et al. Attenuation of $\gamma\delta$ TCR signaling efficiently diversifies thymocytes to the $\alpha\beta$ lineage. *Immunity* (2005) 22:595–606. doi: 10.1016/j.immuni.2005.04.003
- Hayes SM, Li L, Love PE. TCR signal strength influences $\alpha\beta/\gamma\delta$ lineage fate. *Immunity* (2005) 22:583–93. doi: 10.1016/j.immuni.2005.03.014
- Joachims ML, Chain JL, Hooker SW, Knott-Craig CJ, Thompson LF. Human $\alpha\beta$ and $\gamma\delta$ thymocyte development: TCR gene rearrangements, intracellular TCR β expression, and $\gamma\delta$ developmental potential - differences between men and mice. *J Immunol* (2006) 176:1543–52. doi: 10.4049/jimmunol.176.3.1543
- Rodríguez-Caparrós A, García V, Casal Á, López-Ros J, García-Mariscal A, Tani-ichi S, et al. Notch signaling controls transcription via the recruitment of RUNX1 and MYB to enhancers during thymocyte development. *J Immunol* (2019) 202:2460–72. doi: 10.4049/jimmunol.1801650
- Ferrero I, Mancini SJ, Grosjean F, Wilson A, Otten L, MacDonald HR. TCR γ silencing during $\alpha\beta$ T cell development depends upon pre-TCR-induced proliferation. *J Immunol* (2006) 177:6038–43. doi: 10.4049/jimmunol.177.9.6038
- Tani-ichi S, Satake M, Ikuta K. The pre-TCR signal induces transcriptional silencing of the TCR γ locus by reducing the recruitment of STAT5 and runx to transcriptional enhancers. *Int Immunol* (2011) 23:553–63. doi: 10.1093/intimm/dxr055
- Erman B, Feigenbaum L, Coligan JE, Singer A. Early TCR α expression generates TCR $\alpha\gamma$ complexes that signal the DN-to-DP transition and impair development. *Nat Immunol* (2002) 3:564–9. doi: 10.1038/ni800
- Abarrategui I, Krangel MS. Regulation of T cell receptor- α gene recombination by transcription. *Nat Immunol* (2006) 7:1109–15. doi: 10.1038/ni1379
- Abarrategui I, Krangel MS. Noncoding transcription controls downstream promoters to regulated T-cell receptor α recombination. *EMBO J* (2007) 26:4380–90. doi: 10.1038/sj.emboj.7601866
- Ji Y, Little AJ, Banerjee JK, Hao B, Oltz EM, Krangel MS, et al. Promoters, enhancers, and transcription target RAG1 binding during V(D)J recombination. *J Exp Med* (2010) 207:2809–16. doi: 10.1084/jem.20101136
- Klein F, Mitrovic M, Roux J, Engdahl C, von Muenchow L, Alberti-Servera L, et al. The transcription factor duxb1 mediates elimination of pre-t-cells that fail β -selection. *J Exp Med* (2019) 216:638–55. doi: 10.1084/jem.20181444
- Xiong N, Kang C, Raulet DH. Redundant and unique roles of two enhancer elements in the TCR γ locus in gene regulation and $\gamma\delta$ T cell development. *Immunity* (2002) 16:453–63. doi: 10.1016/s1074-7613(02)00285-6
- Monroe RJ, Sleckman BP, Monroe BC, Khor B, Claypool S, Ferrini R, et al. Developmental regulation of TCR δ locus accessibility and expression by the TCR δ enhancer. *Immunity* (1999) 10:503–13. doi: 10.1016/s1074-7613(00)80050-3
- Rothenberg EV, Ungerback J, Champhekar A. Forging T-lymphocyte identity: intersecting networks of transcriptional control. *Adv Immunol* (2016) 129:109–74. doi: 10.1016/bs.ai.2015.09.002
- Radtke F, Fasnacht N, MacDonald HR. Notch signaling in the immune system. *Immunity* (2010) 32:14–27. doi: 10.1016/j.immuni.2010.01.004
- Moore T, von Freeden-Jeffry U, Murray R, Zlotnik A. Inhibition of $\gamma\delta$ T cell development and early thymocyte maturation in IL-7 $^{-/-}$ mice. *J Immunol* (1996) 157:2366–73.
- Maki K, Sunaga S, Komagata Y, Kodaira Y, Mabuchi A, Karasuyama K, et al. Interleukin 7 receptor-deficient mice lack $\gamma\delta$ T cells. *Proc Natl Acad Sci USA* (1996) 93:7172–7. doi: 10.1073/pnas.93.14.7172
- Boudil A, Matei IR, Shih H-Y, Bogdanoski G, Yuan JS, Chang SG, et al. IL-7 coordinates proliferation, differentiation and *Tcr* recombination during thymocyte β -selection. *Nat Immunol* (2015) 16:397–405. doi: 10.1038/ni.3122
- Nakamura M, Shibata K, Hatano S, Sato T, Ohkawa Y, Yamada H, et al. A genome-wide analysis identifies a notch-RBPJc-IL-7R α axis that controls IL-17-producing $\gamma\delta$ T cell homeostasis in mice. *J Immunol* (2014) 194:243–51. doi: 10.4049/jimmunol.1401619
- González-García S, García-Peydró M, Martín-Gayo E, Ballestar E, Esteller M, Bornstein R, et al. CSL-MALM-dependent Notch1 signaling controls lineage-specific IL-7R α gene expression in early human thymopoiesis and leukemia. *J Exp Med* (2009) 206:779–91. doi: 10.1084/jem.20081922
- Wang H, Zang C, Taing L, Arnett KL, Wong YJ, Pear WS, et al. NOTCH1-RBPJ complexes drive target gene expression through dynamic interactions with superenhancers. *Proc Natl Acad Sci USA* (2014) 111:705–10. doi: 10.1073/pnas.1315023111
- Yashiro-Ohtani Y, He Y, Ohtani T, Jones ME, Shestova O, Xu L, et al. Pre-TCR signaling inactivates Notch1 transcription by antagonizing E2A. *Genes Dev* (2009) 23:1665–76. doi: 10.1101/gad.1793709
- Hernández-Munain C, Krangel MS. Regulation of the T-cell receptor δ enhancer by functional cooperation between c-myc and core-binding factors. *Mol Cell Biol* (1994) 14:473–83. doi: 10.1128/mcb.14.1.473-483.1994
- Hernández-Munain C, Krangel MS. C-myc and core-binding factor/PEBP2 display functional synergy but bind independently to adjacent sites in the T-cell receptor δ enhancer. *Mol Cell Biol* (1995) 15:3090–9. doi: 10.1128/MCB.15.6.3090
- Hernández-Munain C, Lauzurica P, Krangel MS. Regulation of T cell receptor δ gene rearrangement by c-myc. *J Exp Med* (1996) 183:289–93. doi: 10.1084/jem.183.1.289
- Lauzurica P, Zhong XP, Krangel MS, Roberts JL. Regulation of T cell receptor δ gene rearrangement by CBF/PEBP2. *J Exp Med* (1997) 185:1193–201. doi: 10.1084/jem.185.7.1193
- Hsiang YH, Goldman JP, Raulet DH. The role of c-myc or a related factor in regulating the T cell receptor γ gene enhancer. *J Immunol* (1995) 154:5195–204.
- Maki K, Sunaga S, Ikuta K. The V-J recombination of T cell receptor- γ genes is blocked in interleukin-7 receptor-deficient mice. *J Exp Med* (1996) 184:2423–7. doi: 10.1084/jem.184.6.2423
- Ye SK, Agata Y, Lee HC, Kurooka H, Kitamura T, Shimizu A, et al. The IL-7 receptor controls the accessibility of the TCR γ locus by Stat5 and histone acetylation. *Immunity* (2001) 15:813–23. doi: 10.1016/s1074-7613(01)00230-8
- Ye SK, Maki K, Kitamura T, Sunaga S, Akashi K, Domen J, et al. Induction of germline transcription of the TCR γ locus by Stat5: implications for accessibility control by the IL-7 receptor. *Immunity* (1999) 11:213–23. doi: 10.1016/s1074-7613(00)80096-5
- Lee H-C, Ye S-K, Honjo T, Ikuta K. Induction of germline transcription in the human TCR γ locus by STAT5. *J Immunol* (2001) 167:320–6. doi: 10.4049/jimmunol.167.1.320
- Candéias S, Peschon JJ, Muegge K, Durum SK. Defective T-cell receptor γ gene rearrangement in interleukin-7 receptor knockout mice. *Immunol Lett* (1997) 57:9–14. doi: 10.1016/s0165-2478(97)00062-x
- Schlissel MS, Durum SD, Muegge K. The interleukin 7 receptor is required for T cell receptor γ locus accessibility to the V(D)J recombinase. *J Exp Med* (2000) 191:1045–50. doi: 10.1084/jem.191.6.1045
- Tani-ichi S, Satake M, Ikuta K. Activation of the mouse TCR γ enhancers by STAT5. *Int Immunol* (2009) 21:1079–88. doi: 10.1093/intimm/dxp073

45. Masui N, Tani-ichi S, Maki K, Ikuta K. Transcriptional activation of mouse TCR γ J γ 4 germline promoter by STAT5. *Mol Immunol* (2008) 45:849–55. doi: 10.1016/j.molimm.2007.06.157
46. Maki K, Ikuta K. MEK1/2 induces STAT5-mediated germline transcription of the TCR γ locus in response to IL-7R signaling. *J Immunol* (2008) 181:494–502. doi: 10.4049/jimmunol.181.1.494
47. Wagatsuma K, Tani-ichi S, Liang B, Shitara S, Ishihara K, Abe M, et al. STAT5 orchestrates local epigenetic changes for chromatin accessibility and rearrangements by direct binding to the TCR γ locus. *J Immunol* (2015) 195:1804–14. doi: 10.4049/jimmunol.1302456
48. Kang J, Coles M, Raulet DH. Defective development of $\gamma\delta$ T cells in interleukin 7 receptor-deficient mice is due to impaired expression of T cell receptor γ genes. *J Exp Med* (1999) 190:973–82. doi: 10.1084/jem.190.7.973
49. Shinkai Y, Rathbun G, Lam P, Oltz EM, Stewart V, Mendelsohn M, et al. RAG-2-deficient mice lack mature lymphocytes owing to inability to initiate V(D)J recombination. *Cell* (1992) 68:855–67. doi: 10.1016/0092-8674(92)90029-c
50. Carleton M, Ruetsch NR, Berger MA, Rhodes M, Kaptik S, Wiest DL. Signals transduced by CD3 ϵ , but not by surface pre-TCR complexes, are able to induce maturation of an early thymic lymphoma *in vitro*. *J Immunol* (1999) 163:2576–85.
51. Anderson MK, Weiss AH, Hernández-Hoyos G, Dionne CJ, Rothenberg EV. Constitutive expression of PU.1 fetal hematopoietic progenitors block T cell development at the pro-T cell stage. *Immunity* (2002) 16:285–96. doi: 10.1016/s1074-7613(02)00277-7
52. Dionne CJ, Tse KY, Weiss AH, Franco CB, Wiest DL, Anderson MK, et al. Subversion of T lineage commitment by PU.1 in a clonal cell line system. *Dev Biol* (2005) 280:448–66. doi: 10.1016/j.ydbio.2005.01.027
53. Alves NL, van Leeuwen EM, Derks IA, van Lier RA. Differential regulation of human IL-7 receptor α expression by IL-7 and TCR signaling. *J Immunol* (2008) 180:5201–10. doi: 10.4049/jimmunol.180.8.5201
54. Aster JC, Xu L, Karnell FG, Patriub V, Pui JC, Pear WS. Essential roles for ankyrin repeat and transactivation domains in induction of T-cell leukemia by notch1. *Mol Cell Biol* (2000) 20:7505–15. doi: 10.1128/MCB.20.20.7505-7515.2000
55. Simandi Z, Horvath A, Nagy P, Nagy L. Prediction and validation of gene regulatory elements activated during retinoic induced embryonic stem cell differentiation. *J Vis Exp* (2016) 112:53978. doi: 10.3791/53978
56. Redondo JM, Pfohl JL, Krangel MS. Identification of an essential site for transcriptional activation within human T-cell receptor δ enhancer. *Mol Cell Biol* (1991) 11:5671–80. doi: 10.1128/mcb.11.11.5671
57. Heng TSP, Painter MW. The Immunological Genome Project Consortium. The immunological genome project: networks of gene expression in immune cells. *Nat Immunol* (2008) 9:1091–4. doi: 10.1038/ni1008-1091
58. Proudhon C, Snetkova V, Raviram R, Lobry C, Badry S, Jiang T, et al. Active and inactive enhancers cooperate to exert localized and long-range control of gene regulation. *Cell Rep* (2016) 15:2159–69. doi: 10.1016/j.celrep.2016.04.087
59. del Blanco B, Angulo Ú, Krangel MS, Hernández-Munain C. The *Tcr α* enhancer is inactivated in $\alpha\beta$ T lymphocytes. *Proc Natl Acad Sci USA* (2015) 112:1744–53. doi: 10.1073/pnas.1406551112
60. del Blanco B, García-Mariscal A, Wiest DL, Hernández-Munain C. *Tcr α* enhancer activation by inducible transcription factors downstream of pre-TCR signaling. *J Immunol* (2012) 188:3278–93. doi: 10.4049/jimmunol.1100271
61. Carabaña J, Ortigoza E, Krangel MS. Regulation of the murine D δ 2 promoter by upstream stimulatory factor 1, Runx1, and c-myb. *J Immunol* (2005) 174:4144–52. doi: 10.4049/jimmunol.174.7.4144
62. Bosma GC, Custer RP, Bosma MJ. A severe combined immunodeficiency mutation in the mouse. *Nature* (1983) 301:527–30. doi: 10.1038/301527a0
63. Carleton M, Haks MC, Smeel SAA, Jones A, Belkowski SM, Berger MA, et al. Early growth response transcription factors are required for development of CD4⁺CD8⁺ thymocytes to the CD4⁺CD8⁺ stage. *J Immunol* (2002) 168:1649–58. doi: 10.4049/jimmunol.168.4.1649
64. Laurent J, Bosco N, Marche PN, Ceredig R. New insights into the proliferation and differentiation of early mouse thymocytes. *Int Immunol* (2004) 16:1069–80. doi: 10.1093/intimm/dxh108
65. Zhu Y, Sun L, Chen Z, Whitaker JW, Wang T, Wang W. Predicting enhancer transcription and activity from chromatin modifications. *Nucleic Acids Res* (2013) 41:10032–43. doi: 10.1093/nar/gkt826
66. Sartorelli V, Lauberth SM. Enhancer RNAs are important regulatory layer of epigenome. *Nat Struct Mol Biol* (2020) 27:521–8. doi: 10.1038/s41594-020-0446-0
67. Pekowska A, Benoukraf T, Zacarias-Cabeza J, Belhocine M, Koch F, Holota H, et al. H3K4 tri-methylation provides an epigenetic signature of active enhancers. *EMBO J* (2011) 30:4198–210. doi: 10.1038/emboj.2011.29
68. Creighton MP, Cheng AW, Welstead GG, Kooistra T, Carey BW, Steine EJ, et al. Histone H3K27ac separates active from poised enhancers and predicts developmental state. *Proc Natl Acad Sci USA* (2010) 107:21931–6. doi: 10.1073/pnas.1016071107
69. Hernández-Munain C, Sleckman BP, Krangel MS. A developmental switch from TCR δ enhancer to TCR α enhancer function during thymocyte maturation. *Immunity* (1999) 10:723–33. doi: 10.1016/s1074-7613(00)80071-0
70. Ashworth TD, Pear WS, Chiang MY, Blacklow SC, Mastio J, Xu L, et al. Deletion-based mechanisms of Notch1 activation in T-ALL: key roles for RAG recombinase and a conserved internal translational start site in Notch1. *Blood* (2010) 116:5455–64. doi: 10.1182/blood-2010-05-286328
71. Del Real MM, Rothenberg EV. Architecture of a lymphomyeloid developmental switch controlled by PU.1, notch and Gata3. *Development* (2013) 140:1207–19. doi: 10.1242/dev.088559
72. Kaikonen MU, Spann NJ, Heinz S, Romanoski CE, Allison KA, Stender JD, et al. Remodeling of the enhancer landscape during macrophage activation is coupled to enhancer transcription. *Mol Cell* (2013) 51:310–25. doi: 10.1016/j.molcel.2013.07.010
73. Arnold PR, Wells AD, Li XC. Diversity and emerging roles of enhancer RNA in regulation of gene expression and cell fate. *Front Cell Dev Biol* (2020) 7:377. doi: 10.3389/fcell.2019.00377
74. Pefanis E, Wang J, Rothschild G, Lim J, Kazadi D, Sun J, et al. RNA Exosome-regulated non-coding RNA transcription controls super-enhancer activity. *Cell* (2015) 161:774–89. doi: 10.1016/j.cell.2015.04.034
75. Chen L, Carico Z, Shih H-Y, Krangel MS. A discrete chromatin loop in the mouse *Tcr α -Tcr δ* locus shapes the TCR δ and TCR α repertoires. *Nat Immunol* (2015) 16:1085–93. doi: 10.1038/ni.3232
76. Sleckman BP, Bardon CG, Ferrini R, Davidson L, Alt FW. Function of the TCR α enhancer in $\alpha\beta$ and $\gamma\delta$ T cells. *Immunity* (1997) 7:505–15. doi: 10.1016/s1074-7613(00)80372-6
77. Aifantis I, Bassing CH, Garbe AI, Sawai K, Alt FW, von Boehmer H. The $\epsilon\delta$ enhancer controls the generation of CD4⁺CD8⁺ $\alpha\beta$ TCR-expressing T cells that can give rise to different lineages of $\alpha\beta$ T cells. *J Exp Med* (2006) 203:1543–50. doi: 10.1084/jem.20051711
78. Rodríguez-Caparrós A, Álvarez-Santiago J, López-Castellanos L, Ruiz-Rodríguez C, Valle-Pastor MJ, López-Ros J, et al. Differently regulated gene-specific activity of enhancers located at the boundary of sub-topologically associated domains: TCR α enhancer. *J Immunol* (2022) 208:910–28. doi: 10.4049/jimmunol.2000864
79. King DM, Hong CKY, Shepherdson JL, Granas DM, Maricque BB, Cohen BA. Synthetic and genomic regulatory elements reveal aspects of *cis*-regulatory grammar in mouse embryonic stem cells. *eLife* (2020) 9:e41279. doi: 10.7554/eLife.41279
80. Vandel J, Cassan O, Lèbre S, Lecellier C-H, Bréhélin L. Probing transcription factor combinatorics in different promoter classes and in enhancers. *BMC Genomics* (2019) 20:103. doi: 10.1186/s12864-018-5408-0
81. Kuhnert F. Pre-T cell receptor signaling drives leukemogenesis and is a therapeutic target in T cell acute lymphoblastic leukemia. *Hematol Oncol* (2019) 37:365–6. doi: 10.1002/hon.30_2631
82. van Vlierberghe P, Ferrando A. The molecular basis of T cell acute lymphoblastic leukemia. *J Clin Invest* (2012) 122:3398–406. doi: 10.1172/JCI61269
83. Aifantis I, Raetz E, Buonamici S. Molecular pathogenesis of T-cell leukaemia and lymphoma. *Nat Rev Immunol* (2008) 8:380–90. doi: 10.1038/nri2304
84. Larmonie NSD, Dik WA, Meijerink JPP, Homminga I, van Dongen JJM, Langerak AW. Breakpoint sites disclose the role of V(D)J recombination machinery in the formation of T-cell receptor (TCR) and non-TCR associated aberrations in T-cell acute lymphoblastic leukemia. *Hematologica* (2013) 98:1173–84. doi: 10.3324/haematol.2012.082156
85. Le Noir S, Abdelali RB, Lelorch M, Bergeron J, Sungalee S, Payet-Bornet D, et al. Extensive molecular mapping of TCR α/δ - and TCR β -involved chromosomal translocations reveals distinct mechanisms of oncogene activation in T-ALL. *Blood* (2012) 120:3298–309. doi: 10.1182/blood-2012-04-425488

Glossary

ATAC-seq	assay for transposase-accessible chromatin using sequencing
cCRE	candidate <i>cis</i> -regulatory element
C δ	TCR δ gene constant region
cfosp	<i>Fos</i> promoter
C γ	TCR γ gene constant region
ChIP-seq	chromatin immunoprecipitation using sequencing
DAPT	7(B-(35-difluorophenyl)-1-alanyl)-s-phenyl-glycine t-butyl ester
DN	double-negative
DP	double-positive
E δ	TCR δ gene enhancer
E γ	TCR γ gene enhancer
EMSA	electrophoretic mobility shift assay
eRNA	enhancer transcripts
H3K4me3	trimethylated lysine 4 of histone H3
H3K27ac	acetylated lysine 27 of histone H3
ICN1	intracellular NOTCH1 domain
IL-7	interleukin-7
IL-7R	interleukin-7 receptor
qChIP	quantitative chromatin immunoprecipitation
qPCR	quantitative polymerase chain reaction
RNA-seq	transcriptome analysis using sequencing
RT-qPCR	quantitative reverse transcription PCR
SEM	standard error of the mean
SP	single-positive
TCR	T-cell receptor
TCR δ	T-cell receptor δ chain
TCR γ	T-cell receptor γ chain
V δ 1p	TRAV1 promoter